



# Pharmacological Ischemic Conditioning with Roxadustat Does Not Affect Pain-Like Behaviors but Mitigates Sudomotor Impairment in a Murine Model of Deep Hind Paw Incision

Fanglin Lu <sup>1,2</sup>, Jungo Kato<sup>2</sup>, Tomoko Toramaru<sup>2</sup>, Mengting Zhang<sup>1,2</sup>, Hiroshi Morisaki <sup>2</sup>

<sup>1</sup>Keio University Graduate School of Medicine Doctoral Programs, Tokyo, Japan; <sup>2</sup>Department of Anesthesiology, Keio University School of Medicine, Tokyo, Japan

Correspondence: Jungo Kato, Department of Anesthesiology, Keio University School of Medicine, 35 Shinanoamchi, Shinjuku-ku, Tokyo, 160-8582, Japan, Tel +81-3-3353-1211, Fax +81-3-3356-8439, Email jungo-k.a2@keio.jp

**Purpose:** The involvement of hypoxic response mechanisms in local functional impairments in surgical wounds is unclear. In the present study, we characterized tissue hypoxia in surgical wounds and investigated the role of pharmacological ischemic conditioning (PIC) using roxadustat, an oral prolyl hydroxylase domain enzyme inhibitor, in postoperative local functional impairments in a murine model of deep hind paw incision.

**Methods:** Male BALB/cAJcl mice aged 9–13 weeks were used in all experiments. Plantar skins of mice that underwent surgical incision were subjected to immunohistochemistry to localise tissue hypoxia. Pain-like behaviours and sudomotor function were compared between mice treated with 6-week perioperative PIC and control mice. The effects of PIC were examined in vitro by immunocytochemistry using sympathetically differentiated PC12 cells and in vivo by immunohistochemistry using plantar skins collected on postoperative day 21.

**Results:** Prominent tissue hypoxia was detected within axons in the nerve bundles underneath surgical wounds. Six-week perioperative PIC using roxadustat failed to ease spontaneous pain-like behaviors; however, it mitigated local sudomotor impairment post-operatively. Upregulation of sympathetic innervation to the eccrine glands was observed in the PIC-treated skins collected on postoperative day 21, in accordance with the in vitro study wherein roxadustat promoted neurite growth of sympathetically differentiated PC12 cells.

**Conclusion:** This study suggests that tissue hypoxia is involved in the pathogenesis of local sudomotor dysfunction associated with surgical trauma. Targeting the hypoxic response mechanisms with PIC may be of therapeutic potential in postsurgical local sympathetic impairments that can be present in complex regional pain syndrome.

**Keywords:** complex regional pain syndrome, hypoxic response mechanisms, postoperative pain, sudomotor dysfunction, sympathetic denervation

## Plain Language Summary

Pain after surgery is a common complaint by many patients. This pain is triggered by low oxygen concentration and accumulation of lactate and reactive oxygen species in the surgical wound. The present study was performed to examine the therapeutic potential of pharmacological ischemic conditioning (PIC) in local impairments associated with surgical trauma. Using a murine model of deep hind paw incision, the localization of tissue hypoxia and changes in the expression pattern of prolyl hydroxylase domain protein 2 in surgical wounds were examined. Also, the study aimed to examine the effect of perioperative administration of roxadustat, a PIC agent, on pain-like behaviors. Following the study, PIC did not reduce the pain-like behaviors but it alleviated local sweating dysfunction. This means that PIC can be important in targeting hypoxic response mechanisms that can relieve the local sympathetic impairments. Thus, administration of PIC before surgery may have therapeutic potential to improve the clinical outcomes of patients undergoing surgery.

## Introduction

Postoperative pain remains a major clinical problem affecting more than 300 million patients annually worldwide.<sup>1</sup> It frequently persists even beyond the wound healing process.<sup>2</sup> Moreover, surgical insults occasionally lead to complex regional pain syndrome (CRPS), a widely known complication of surgeries on the extremities, which is characterized by a variable combination of sensory, vasomotor, and sudomotor symptoms.<sup>3</sup> Currently, no pharmacological intervention has proven to be clinically effective specifically in preventing chronic postoperative pain.<sup>4</sup> Although massive progress has been made at the bench in unveiling the pathophysiology of chronic pain,<sup>5–8</sup> further identification of different pathways is still necessary to develop effective therapeutic approaches against this multifactorial problem.

Accumulating evidence has suggested the occurrence of tissue hypoxia in surgical wounds, with reduced tissue oxygen tension and pH, as well as increased levels of lactate and reactive oxygen species (ROS).<sup>9,10</sup> These hypoxic changes reportedly exacerbate postoperative pain via activation of nociceptors in the peripheral nervous system (PNS).<sup>11,12</sup> Meanwhile, local tissue hypoxia in surgical sites may also contribute to CRPS development postoperatively.<sup>13</sup>

In vital organs, such as the brain and heart, cells are equipped with hypoxic response machinery against hypoxic insults through the activities of hypoxia-inducible factors (HIFs) and their regulators, the prolyl hydroxylase domain (PHDs) enzymes. During hypoxia, prolyl hydroxylase domain protein 2 (PHD2), a predominant isoform of PHDs ubiquitously expressed in the body, fails to mediate the degradation of hypoxia-inducible factor 1- $\alpha$  (HIF-1 $\alpha$ ). Consequently, HIF-1 $\alpha$ , the key transcriptional regulator in the hypoxic response pathways, can translocate to the nucleus to modulate the expression of adaptive genes, including vascular endothelial growth factor and erythropoietin, which kick-start adaptive responses to hypoxia.<sup>14</sup> However, the pathophysiological roles of these hypoxic response mechanisms in surgery-induced functional impairments, such as postoperative pain and local autonomic dysfunction, remain elusive.

Pharmacological ischemic conditioning (PIC) targeting the activation of hypoxic response pathways, such as the administration of HIF stabilizers (eg, roxadustat, an oral PHD active-site blocker), is able to combat subsequent severe ischemic insults in vital organs in animal models.<sup>15–17</sup> Considering the development of profound tissue hypoxia in surgical wounds, PIC might also aid in managing local functional impairments in surgical wounds. In contrast, excessive activation of hypoxic response pathways might lead to maladaptive consequences, such as progression to chronic postoperative pain or postoperative CRPS.

First, we collectively characterized the localization of tissue hypoxia and changes in the expression pattern of PHD2 in surgical wounds in a murine model of deep hind paw incision. Second, we investigated the effect of PIC using roxadustat on local functional impairments in surgical wounds by focusing on spontaneous pain-like behaviors and sudomotor function. Additionally, we explored the *in vitro* and *in vivo* mechanistic insights of PIC.

## Materials and Methods

### Animals

In this study, 9–13-week-old male BALB/cAJcl mice weighing 25–32 g (CLEA Japan, Inc. Tokyo, Japan; RRID: MGI:2160349) were used in all experiments. All animals were housed in standard cages (four to five per cage) at an ambient temperature of 22°C with a 12:12-h light–dark cycle and fed *ad libitum*. Mice were allowed to acclimatize in laboratory facilities at least 1 week before experimentation. The exclusion criteria included the presence of severe non-surgery-related wounds, signs of systemic weakness (eg, significant weight loss [ $>20\%$  of body weight] and lethargic appearance), and signs of surgical site infection. However, none of the mice recruited in the current study met these criteria. Randomization was performed in each group allocation based on the baseline body weight and weight distribution on the ipsilateral paw in dynamic weight-bearing (DWB) using the current study's custom-made Excel macroprogram. The current study was exploratory and not pre-registered; nonetheless, all experiments were approved by the Keio University Institutional Animal Care and Use Committee, Tokyo, Japan (approval number 11050-2).

All experimental procedures adhered to the Institutional Guidelines on Animal Experimentation at Keio University (<https://www.animal.med.keio.ac.jp/img/kitei.pdf>) and were reported according to the Animal Research: Reporting of In Vivo Experiments (ARRIVE) guidelines. As one of the purposes of the study described in this manuscript was to evaluate the postoperative pain-like behavior, no analgesics were used during behavioral tests to prevent distortion of the

results. Drug administration, behavioral tests, and histological and imaging analyses were performed by experimenters blinded to the experimental allocation.

## Deep Hind Paw Incision Model

The deep hind paw incision was performed, as described previously,<sup>18</sup> with several modifications. The animal was placed in a prone position under sevoflurane anesthesia (4 volume% in 1 L/min oxygen) delivered via a nose cone. Sevoflurane inhalation was used, as it is safe, non-invasive, rapid, and easy to control. Adequate anesthetic depth was ascertained by loss of response to tail clamp. A drape was placed after disinfection with 10% povidone–iodine solution (popiyodon solution 10%; Yoshida Pharmaceutical Co., Ltd., Saitama, Japan). A 5-mm longitudinal incision was made through the skin using a scalpel blade, starting 2 mm from the proximal edge of the heel and extending toward the toe. The underlying fascia and plantaris muscle were incised and elevated for 5 min. After hemostasis, the wound was closed using a 6–0 nylon suture and covered with bacitracin ointment (baramycin ointment; TOYO Pharmaceutical Co., Ltd., Osaka, Japan; catalog number: 672639) to prevent wound infection. Then, the animal was placed in a recovery cage. Once the animal was fully recovered as it regained the righting reflex and ability to stand, it was returned to its home cage. Respiratory patterns and reactions to surgical stimulation were continuously monitored during the entire surgical procedure.

The sham surgery comprised anesthesia, antiseptic preparation, and application of topical antibiotics without skin and muscle incision and elevation (protocol: <http://dx.doi.org/10.17504/protocols.io.j8nlkw9k515r/v1>).

## Drug Administration

Roxadustat (FG-4592; Selleck Chemicals, Osaka, Japan; catalog number: S1007) was dissolved at a volume of 10 mL/kg body weight in an aqueous vehicle containing 5% dimethyl sulfoxide (Tokyo Chemical Industry, Tokyo, Japan; catalog number: D0798), 50% polyethylene glycol 300 (Tokyo Chemical Industry; catalog number: H0543), and 45% distilled water by volume. Based on a previous pharmacological study in mice,<sup>19</sup> vehicle or 12.5 mg/kg body weight (low-dose) or 50 mg/kg body weight (high-dose) roxadustat was administered by oral gavage thrice per week for 3 weeks pre- and postoperatively. Surgery and tissue sample collection were performed 30 min after the animals received their administration on day 21 and day 42, respectively. All drug administrations were performed at approximately 9:00 AM to ensure that circadian rhythms were not affected.

## Behavioral Test

### DWB System to Assess Spontaneous Pain

Spontaneous limb pain-like behaviors were assessed using an advanced DWB apparatus (Bioseb, Vitrolles, Provence-Alpes-Côte D'Azur, France; catalog number: BIO-DWB-M), wherein changes in the postural equilibrium of each freely moving animal were tracked and analyzed.<sup>20</sup> The animal was placed in a transparent enclosure for 1 min for acclimatization, followed by a 5-min recording. A matrix comprising pressure sensors capturing the weight distribution data of each of the four paws was embedded in the floor. Each freely moving animal was filmed from above, and changes in postural equilibrium were synchronously and automatically tracked and analyzed by the software. A zone was considered valid when the following parameters were detected:  $\geq 0.8$  g on one captor with a minimum of two adjacent captors recording  $\geq 1.0$  g. A time segment was considered valid if  $\geq 3$  stable pictures were detected. An observer manually validated each automatically presumed paw position to avoid error identification afterward. Weight distribution toward the ipsilateral paw over the total body weight and paw print area ratio of the ipsilateral paw to the contralateral paw were used as the parameter. Behavioral tests were performed and analyzed by the same experimenter. The test was performed at approximately 11:00 AM to ensure that circadian rhythms were not affected (protocol: <http://dx.doi.org/10.17504/protocols.io.eq2ly76pmlx9/v1>).

## Paw Thickness and Paw Temperature

The ipsilateral hind paws' thickness was measured using a digital caliper (A&D Company, Tokyo, Japan) at the metatarsal level in the dorsal–plantar axis to monitor the degree of paw swelling postoperatively. The temperature of

the ipsilateral hind paws was measured using an infrared rodent thermometer (Bioseb; catalog number: BIO-IRB153). The measurements were performed at approximately 11:00 AM to ensure that circadian rhythms were not affected.

## Sweating Assays

### Starch-Iodine Test

To assess restraint stress-induced sweating, the animal was immobilized in a self-made restraint tube on day 41 at approximately 11:00 AM. Moreover, 10% povidone-iodine solution (Yoshida Pharmaceutical Co., Ltd.) was applied to the plantar surface of bilateral hind paws with a cotton bud. Once dry, the skin surface was coated with a suspension of 100% starch-castor oil (1 g starch per 1 mL castor oil; FUJIFILM Wako Pure Chemical Corp., Osaka, Japan; catalog number: 193-09925; Sigma-Aldrich, St. Louis, MO; catalog number: 259853). Sweat droplets were visualized as dark-colored spots because of iodine-starch reactions. Changes on footpads were video-recorded for 3 min.

To assess the pharmacological sweating, the animals were placed in the supine position under sevoflurane anesthesia (4 volume% in 1 L/min oxygen) 30 min after their last administration of roxadustat on day 42. After starch-castor oil coating, 100 µg pilocarpine hydrochloride (diluted in 150 µL 0.9% saline; Sigma-Aldrich; catalog number: PHR1493) was injected intraperitoneally. Changes on the footpads were video-recorded for 5 min. The number of dark spots was counted for each paw (protocol: <http://dx.doi.org/10.17504/protocols.io.bp2l69d1klqe/v2>).

## Hematological Analyses

Under sevoflurane anesthesia, 100 µL of blood sample was collected via cardiac puncture. Hemoglobin and hematocrit levels were determined using an EC4+ i-STAT cartridge (Abbott Point of Care Inc., Abbott Park, IL; catalog number: 34330525).

## Immunohistochemistry

Pimonidazole adduct immunohistochemistry was performed to detect tissue hypoxia.<sup>9</sup> Pimonidazole (Hypoxyprobe™-1 Omni Kit; CosmoBio Co., Ltd., Tokyo, Japan) was dissolved at the volume of 10 mL/kg body weight in saline. The animals were intraperitoneally injected with 60 mg/kg body weight pimonidazole at 30 min before sacrifice. Under sevoflurane anesthesia (4 volume% in 1 L/min oxygen), the animals were perfused transcardially with 20 mL of 4% paraformaldehyde phosphate buffer solution (FUJIFILM Wako Pure Chemical Corp.) after 20 mL of saline. Plantar skins of bilateral hind paws were carefully harvested and post-fixed overnight at 4°C and then dehydrated and stored in 20% sucrose (Sigma-Aldrich) in phosphate-buffered saline (PBS). Sections were stored at -30°C until use or directly washed with PBS for 15 min. After permeabilization and blockade of non-specific binding, sections were incubated at 4°C overnight with primary antibodies of pimonidazole, PHD2, neurofilament-heavy (NF-H), tyrosine hydroxylase (TH), lymphocyte antigen 6 complex, locus G + locus C (Ly6G+Ly6C), or aquaporin 5 (AQP5). See full details of antibodies in [Supplementary Table 1](#). After thorough washing, sections were incubated for 2 h at room temperature with secondary antibodies conjugated with Alexa Fluor 488 or 594 (1:500, Thermo Fisher Scientific, Waltham, MA; Jackson ImmunoResearch Laboratories, Inc., West Grove, PA) and mounted with 4',6-diamidino-2-phenylindole (Prolong™ Glass Antiade Moutant with NucBlue™; Thermo Fisher Scientific) on slides. Images were acquired using a fluorescence microscope (EVOS FL; Life Technologies Corp., Carlsbad, CA), and the mean intensities of pimonidazole and PHD2 immunoreactivities were measured using Fiji version 1.53 (National Institutes of Health, Bethesda, MD; RRID: SCR\_002285). For the localization of pimonidazole and PHD2 in the nerve bundles, images were acquired using a confocal laser scanning microscope (FLUOVIEW FV3000; Olympus, Tokyo, Japan; RRID: SCR\_017015).

## AbScale Labeling and Three-Dimensional Imaging

The AbScale clearing method with immunostaining of TH was performed, as described previously.<sup>21</sup> After washing, adaptation, permeabilization, and deScaling using the SCALEVIEW-S Kit (FUJIFILM Wako Pure Chemical Corp.; catalog number: 299-79901), hind paw skin samples were incubated with primary antibody against TH (1:500, Merck, Darmstadt,



Germany) at 37°C for 36–48 h, followed by incubation with secondary antibodies conjugated with Alexa Fluor 594 at 37°C for 36–48 h. After rinsing and refixation, skin samples were cleared and stored in ScaleS4 at 4°C, away from light.

Z-stack images were collected using a light sheet fluorescence microscope (Zeiss Lightsheet Z.1; Carl Zeiss, Jena, Germany; RRID: SCR\_020919). The muscle underneath the skin was removed, and the sample was attached to the capillary with glue. Subsequently, digital images were analyzed and rendered using Imaris software version 9.8 (Bitplane, Zürich, Switzerland; RRID: 007370). In the Surpass panel, the Surface algorithm was applied to measure the mean intensity of TH and render the eccrine glands, whereas the Filament algorithm was used to render and quantify the innervation to the eccrine glands.

## PC12 Cell Culture

The current study used the PC12 (JCRB Cell Bank, Tokyo, Japan; cell number: JCRB0733, RRID: CVCL\_0481) cell line, which is not listed as a commonly misidentified cell line by the International Cell Line Authentication Committee (ICLAC; <http://iclac.org/databases/cross-contaminations/>) and not authenticated in this study. According to the cell line data sheet, the life span of PC12 cells is infinite and the passage number is eight at bank. PC12 cells were cultured on a 60-mm collagen IV-coated dish (Discovery Labware, Inc., Woburn, MA) in RPMI1640 medium (Life Technologies Ltd., Renfrew, UK; catalog number: 11875093), supplemented with 5% fetal bovine serum (Nichirei Biosciences Inc, Tokyo, Japan; catalog number: 171012) and 10% heat-inactivated horse serum (Merck; catalog number: H1138) in a 95% humidified atmosphere with 5% carbon dioxide at 37°C. At 50–60% confluence, the PC12 cells were exposed to 10 ng/mL nerve growth factor (mouse beta-nerve growth factor; Sino Biological, Beijing, China; catalog number: 50385-MNAC) and allowed to sympathetically differentiate into sympathetic neuron-like cells for 2 days. Subsequently, the cells were treated with 10  $\mu$ M roxadustat (FG-4592), 100  $\mu$ M roxadustat, or 1% dimethyl sulfoxide (vehicle) dissolved in the culture medium for 2 days.<sup>19</sup>

## Immunocytochemistry

The cells were fixed with 4% paraformaldehyde PBS for 20 min and washed with PBS. After permeabilization and blockade of non-specific binding, the cells were incubated at 4°C overnight with primary antibodies against HIF-1 $\alpha$  (1:100; GeneTex, Irvine, CA) and TH (1:100; Merck) ([Supplementary Table 1](#)). After washing thoroughly, the cells were incubated for 1 h at 22°C with secondary antibodies conjugated with Alexa Fluor 594 (1:500; Thermo Fisher Scientific). Observations were performed with a fluorescence microscope, and the mean intensity of nuclear HIF-1 $\alpha$  and the mean neurite length were measured using Fiji.

## Statistical Analysis

Data were analyzed using GraphPad Prism 9 software (San Diego, CA; RRID: SCR\_002798) and are represented as mean  $\pm$  standard error of the mean (SEM). A two-way repeated-measures analysis of variance (ANOVA) followed by Šidák's multiple comparisons test and one-way ANOVA followed by Tukey's multiple comparisons tests were performed to compare the mean differences between the corresponding groups. A *P*-value of <0.05 was considered statistically significant. A total of 122 animals were included for the experiments in this study. Based on our preliminary data, at least 18 mice were required for each group to detect significant differences between the two groups in the DWB experiments for the two-way ANOVA test (effect size, 0.4U;  $\alpha$ , 0.05; 1- $\beta$ , 0.8; calculated by G\*Power 4.1; RRID: SCR\_013726).<sup>22</sup>

## Results

### Localization of Tissue Hypoxia and Prolyl Hydroxylase Domain 2 Expression

Prominent tissue hypoxia was detected inside the nerve bundles located near surgical wounds (*P* = 0.008 vs naïve, *P* = 0.039 vs sham, *P* = 0.008 vs contralateral; [Figure 1A–D](#)) on day 1 following the deep hind paw incision. Hypoxia signals were also observed in infiltrated polymorphonuclear neutrophils in surgical wounds ([Supplementary Figure S1](#)).

A drastic upregulation of PHD2 was also evident in the nerve bundles adjacent to surgical wounds (*P* < 0.001 vs naïve, sham, and contralateral; [Figure 2A–C](#)). Confocal microscopy provided precise localization of PHD2 in NF-H-positive large-diameter nerves and TH-positive sympathetic nerves ([Figure 2D and E](#)). Aside from the axons in the

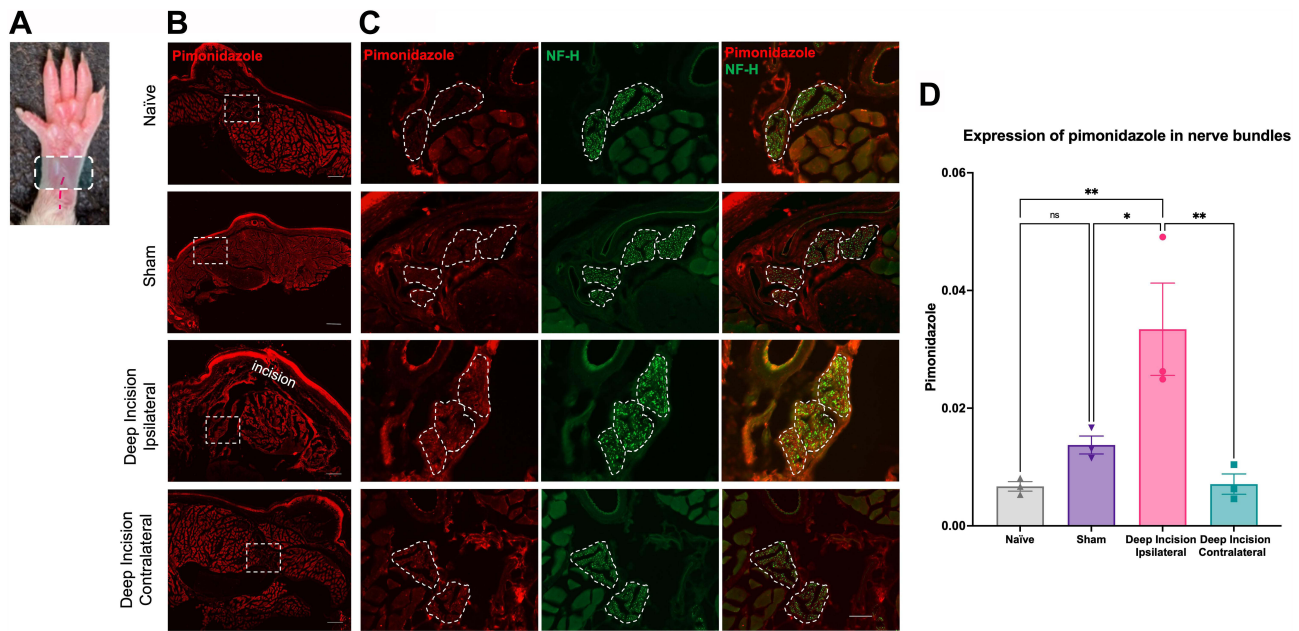


**Figure 1** Tissue hypoxia was detected in the nerve bundles underneath surgical wounds on POD 1. **Notes:** (A) Representative photograph displaying the anatomic location of paw incision (dashed line) and paw sections (dashed box). (B) Representative images of paw sections stained for pimonidazole on POD 1, showing the location of nerve bundles (dashed boxes). Scale bar = 200  $\mu$ m. (C) Representative images of nerve bundles (dashed lines) stained for pimonidazole and NF-H on POD 1. Scale bar = 50  $\mu$ m. (D) Quantification of pimonidazole in the nerve bundles underneath the site of incision on POD 1 (n = 3 per group). Data are expressed as mean  $\pm$  SEM, assessed by one-way ANOVA with Tukey's multiple comparisons test. \* $P < 0.05$ , \*\* $P < 0.01$ . **Abbreviations:** POD, postoperative day; NF-H, neurofilament-heavy; ns, not significant.

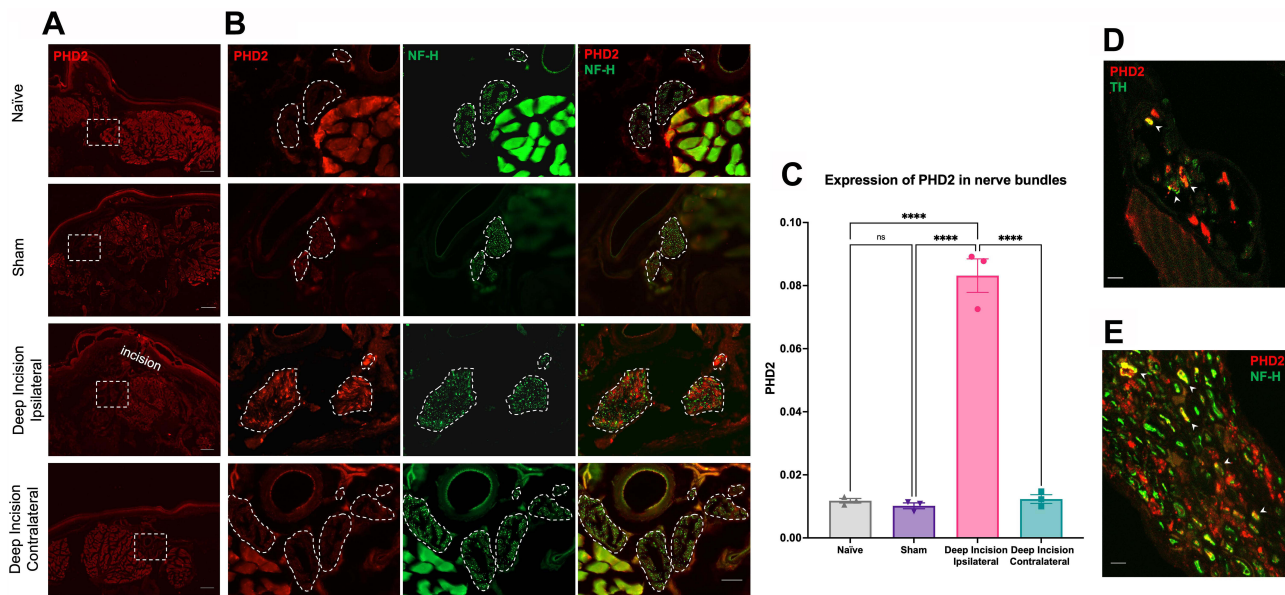


**Figure 2** PHD2 was upregulated within the axons in the nerve bundles underneath surgical wounds on POD 1. **Notes:** (A) Representative images of paw sections stained with PHD2 on POD 1, indicating the location of nerve bundles (dashed boxes). Scale bar = 200  $\mu$ m. (B) Representative images of nerve bundles (dashed lines) displaying immunoreactivities for PHD2 and NF-H on POD 1. Scale bar = 50  $\mu$ m. (C) Quantification of PHD2 in the nerve bundles underneath the site of incision on POD 1 (n = 3 per group). (D and E) Representative confocal microscopy images displaying the localization of PHD2 in the nerve bundles underneath the site of incision. Arrowheads indicate PHD2/TH (D) and PHD2/NF-H (E) colocalization. Scale bar = 5  $\mu$ m. Data are expressed as mean  $\pm$  SEM, assessed by one-way ANOVA with Tukey's multiple comparisons test. \*\*\*\* $P < 0.0001$ . **Abbreviations:** PHD2, prolyl hydroxylase domain protein 2; POD, postoperative day; NF-H, neurofilament-heavy; TH, tyrosine hydroxylase; ns, not significant.

nerve bundles in the glabrous skin, a high intensity of PHD2 signals was observed in eccrine sweat gland cells of both naïve and operated mice ([Supplementary Figure S2](#)).

## Effect of PIC Using Roxadustat on Postoperative Spontaneous Pain-Like Behaviors and Local Sweating Impairment

On the effect of PIC on surgical wound-related sensory and autonomic impairments in behavioral analyses using roxadustat, dose-dependent increases in hemoglobin concentration (main effect factor  $F_{2,15} = 4.397$ ,  $P = 0.031$ ; vehicle vs low-dose roxadustat,  $P = 0.628$ ; vehicle vs high-dose roxadustat,  $P = 0.031$ ; [Figure 3A](#)) and hematocrit level ( $F_{2,15} = 4.496$ ,  $P = 0.030$ ; vehicle vs low-dose roxadustat,  $P = 0.626$ ; vehicle vs high-dose roxadustat,  $P = 0.029$ ; [Figure 3B](#)) after perioperative PIC were observed. The lower dose that represents the clinically recommended dose for renal anemia was selected for the remaining in vivo experiments.<sup>23</sup>

Compared with the vehicle, PIC did not change the time course and severity of paw swelling after incision ([Figure 3C](#)). Similarly, no main effect on spontaneous pain-like behaviors was determined by dynamic weight distribution ( $F_{1,36} = 0.943$ ,  $P = 0.338$ ; [Figure 3D](#)) and paw print area ( $F_{1,36} = 0.819$ ,  $P = 0.371$ ; [Figure 3E](#)) of the operated hind paw was observed after deep hind paw incision between the roxadustat- and vehicle-treated mice. PIC alone without surgery did not affect the outcomes of these parameters ([Supplementary Figure S3](#)).

Altogether, PIC did not significantly affect postoperative local inflammation or pain-like behaviors in our deep hind paw incision model.

In the restraint stress-induced sweating assay performed on postoperative day (POD) 20 (day 41 after the start of PIC), the deep hind paw incision resulted in a significant decline in the sudomotor function of the footpads in the operated hind paw ( $F_{1,25} = 8.389$ ,  $P = 0.008$  vs naïve; [Figure 4A–C](#)). Interestingly, the local sweating impairment was significantly attenuated in the roxadustat-treated mice ( $F_{1,30} = 6.460$ ,  $P = 0.016$  vs vehicle; [Figure 4B and C](#)). No significant difference was observed among all groups in pilocarpine-induced sweating on POD 21, where the muscarinic M3 receptors on eccrine gland cells are directly stimulated ([Figure 4D and E](#)). Additionally, no difference in paw temperature was observed ([Figure 4F](#)). PIC alone without surgery did not affect the outcomes of sweating assays and paw temperatures ([Supplementary Figure S4](#)).

## PIC Using Roxadustat and Sympathetic Neurite Growth

Incubation with roxadustat resulted in a dose-dependent increase in nuclear translocation of HIF-1 $\alpha$  ( $P = 0.042$ , vehicle vs 10  $\mu\text{M}$  roxadustat;  $P = 0.001$ , vehicle vs 100  $\mu\text{M}$  roxadustat; [Figure 5A and B](#)).

Furthermore, roxadustat treatment dose-dependently increased TH-positive sympathetic neurite length ( $P = 0.130$ , vehicle vs 10  $\mu\text{M}$  roxadustat;  $P < 0.001$ , vehicle vs 100  $\mu\text{M}$  roxadustat; [Figure 5C and D](#)).

## Effect of PIC Using Roxadustat on Sympathetic Innervation to the Eccrine Glands

Regarding the in vivo effects of PIC on sympathetic innervation to the eccrine glands by three-dimensional (3D) immunohistochemistry using tissue-cleared skin samples ([Figure 6A](#)), the PIC without surgery did not affect the TH-positive sympathetic innervation around the eccrine glands compared with naïve tissues ([Supplementary Figure S5](#) and [Supplementary Videos S1, S4, and S5](#)). The density of TH-positive sympathetic fibers ( $P = 0.024$  vs naïve; [Figure 6B](#)) and the total lengths of sympathetic fibers around the eccrine glands ( $P = 0.009$  vs naïve; [Figure 6C](#)) and within glands ( $P = 0.029$  vs naïve; [Figure 6D](#)) adjacent to surgical wounds in untreated mice on POD 21 drastically decreased. On the other hand, PIC significantly mitigated the surgery-induced sympathetic denervation ( $P = 0.029$  vs vehicle in the eccrine glands;  $P < 0.001$  vs vehicle in the surrounding nerve;  $P < 0.001$  vs vehicle in whole nerves), to an extent similar to that in naïve mice ([Figure 6B–E](#) and [Supplementary Videos S1, S2, S3](#)).

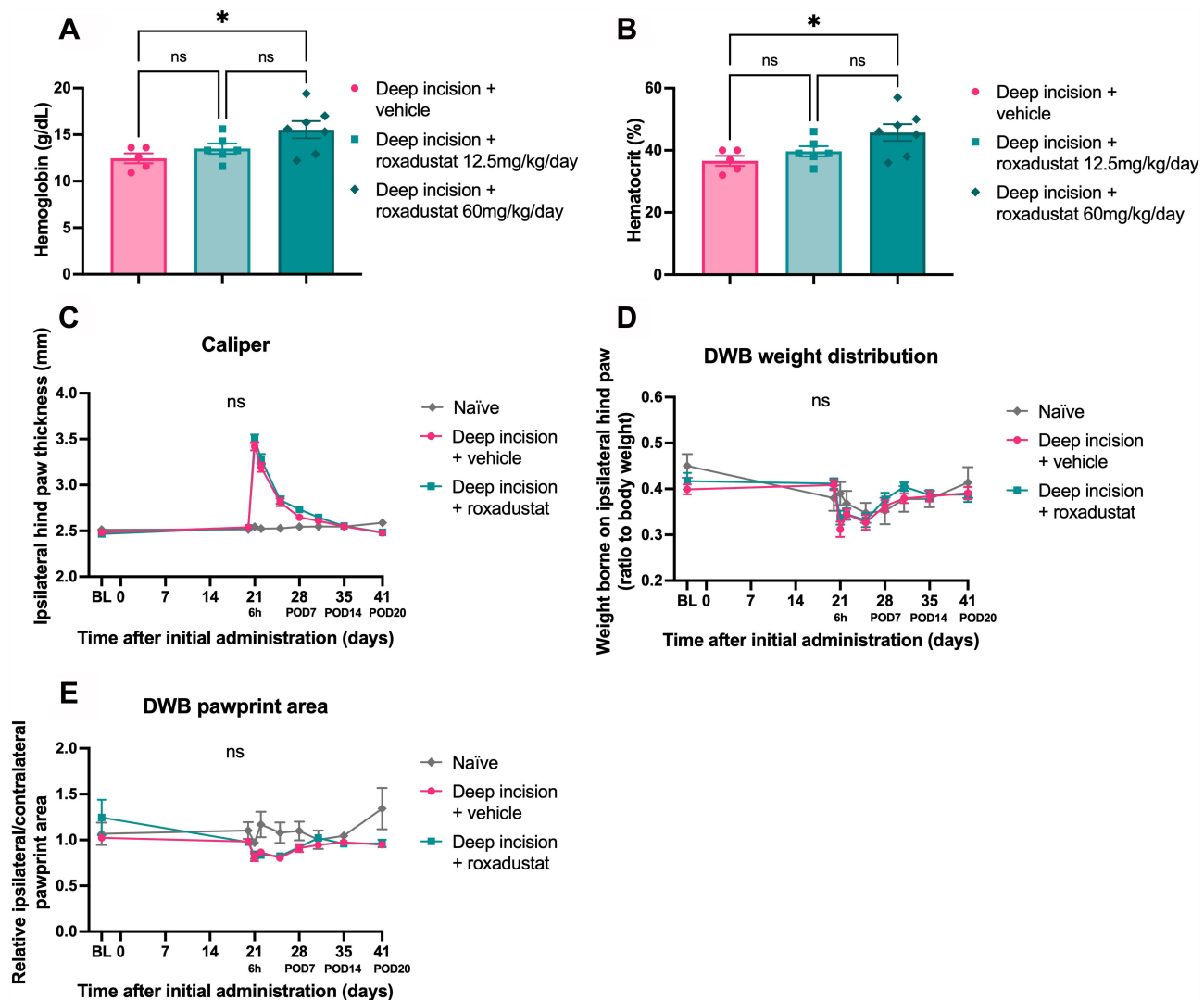


**Figure 3** Effect of PIC on hemoglobin concentration, hematocrit level, postoperative paw swelling and spontaneous pain-like behaviors.

**Notes:** Perioperative PIC using roxadustat dose dependently increased hemoglobin and hematocrit levels. Thus, the lower dose was selected for all in vivo experiments, but it did not significantly affect postoperative local inflammation or pain-like behaviors after deep hind paw incision. Hemoglobin (A) and hematocrit (B) levels after 6 weeks of roxadustat or vehicle administration (3 weeks after deep incision,  $n = 5-7$  per group). Changes in ipsilateral hind paw thickness (C), weight distribution ratio of the ipsilateral paw to the total body weight (D) and paw print area ratio of the ipsilateral paw to the contralateral paw (E) of naïve, deep incision + vehicle and deep incision + roxadustat mice from baseline to POD 20 ( $n = 19$  per group). Data are expressed as mean  $\pm$  SEM, assessed by one-way ANOVA with Tukey's multiple comparisons test (A and B) and two-way ANOVA with Šidák's multiple comparisons test (C-E). \* $P < 0.05$ .

**Abbreviations:** PIC, pharmacological ischemic conditioning; POD, postoperative day; DWB, dynamic weight-bearing; ns, not significant.

## Discussion

Perioperative PIC with roxadustat alleviated the surgery-induced local sudomotor impairment by facilitating sympathetic innervation to the eccrine glands adjacent to surgical wounds. To the best of our knowledge, this is the first report to examine the therapeutic potential of PIC in local impairments associated with surgical trauma.

## Hypoxic Response in Surgical Wounds

Immediately after surgical insult, damaged tissues fall into a hypoxic state,<sup>9</sup> possibly due to vasculature disruption, tissue edema, and resultant impairment of oxygen delivery to the tissues surrounding the wound.<sup>24</sup> High oxygen consumption by infiltrating immune cells (eg, polymorphonuclear neutrophils) may also contribute to tissue hypoxia in surgical wounds.<sup>25</sup> Here, the PNS may be a major victim of local tissue hypoxia after surgical trauma. Consistently, transition to anaerobic glycolysis within the injured peripheral nerves, as evidenced by an elevated lactate level, has been reported in



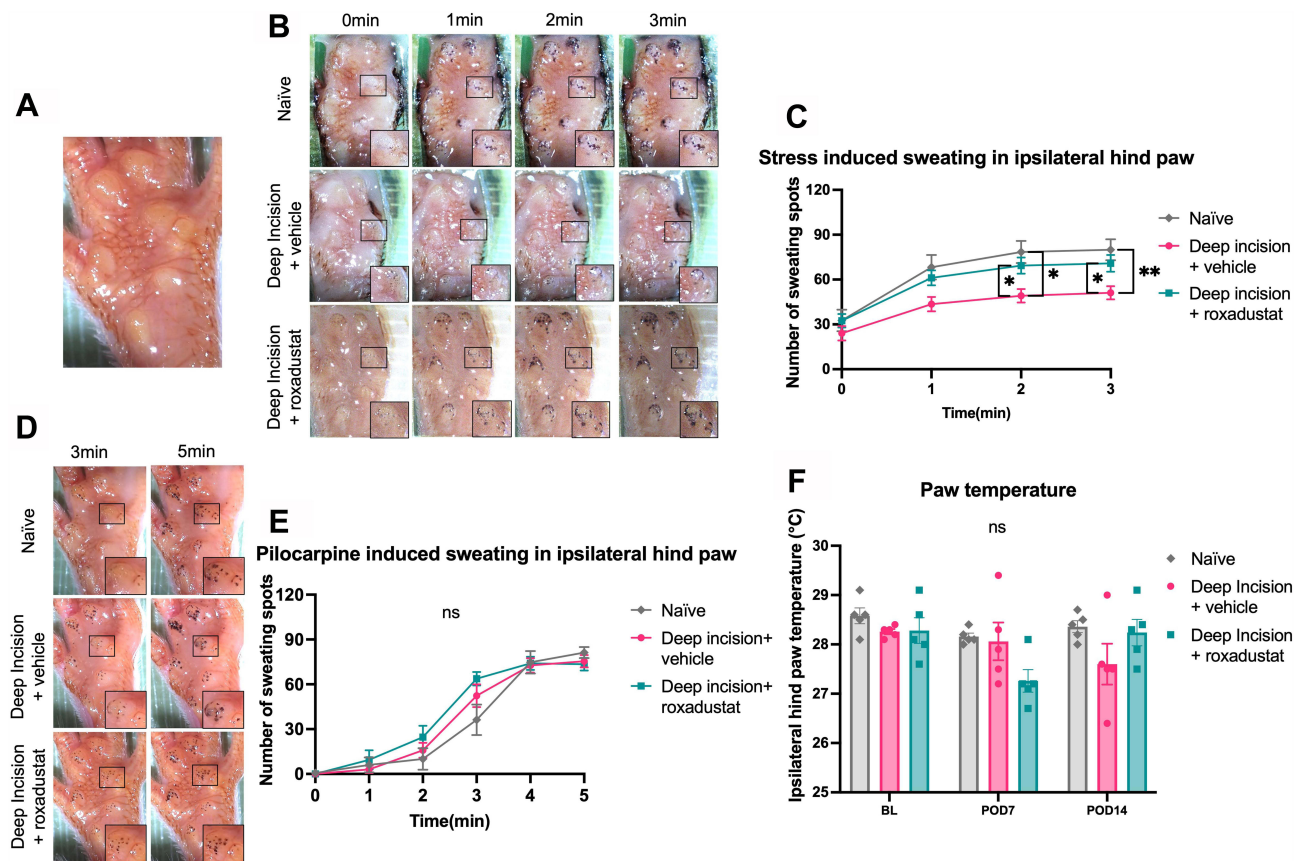


**Figure 4** Perioperative PIC using roxadustat mitigated surgery-induced local sweating impairments in the restraint stress-induced sweating assay, whereas no difference was observed in pilocarpine-induced sweating and paw temperature.

**Notes:** (A) Representative photograph displaying the anatomic location of six footpads on the ipsilateral plantar hind paw. (B) Representative images of sweat droplets on ipsilateral footpads of naïve, deep incision + vehicle, and deep incision + roxadustat mice under restraint stress on POD 20. Inserts indicate a single footpad. (C) Quantification of restraint stress-induced perspiration on POD 20 ( $n = 11-16$  per group). (D) Representative images of sweat droplets on ipsilateral footpads of naïve, deep incision + vehicle, and deep incision + roxadustat mice after administration of pilocarpine on POD 21. Inserts indicate a single footpad. (E) Quantification of pilocarpine-induced perspiration on POD 21 ( $n = 11-15$  per group). (F) Ipsilateral hind paw temperature at baseline, on POD 7, and on POD 14 ( $n = 5$  per group). Data are expressed as mean  $\pm$  SEM, assessed by repeated measures two-way ANOVA followed by Šidák's multiple comparisons test. \* $P < 0.05$ , \*\* $P < 0.01$ .

**Abbreviations:** PIC, pharmacological ischemic conditioning; POD, postoperative day; BL, baseline; ns, not significant.

a murine model of peripheral nerve injury.<sup>26</sup> Moreover, PHD2 was also expressed and upregulated in the damaged peripheral nerves. Considering the previously demonstrated expression of HIF-1 $\alpha$ ,<sup>27</sup> the PNS may be well equipped with hypoxic response machinery.

## PIC and Postoperative Pain

The potential involvement of hypoxic response mechanisms in the regulation of nociception has been controversial. PHD inhibition augments the sensitivity of TRPA1 to ROS in the sensory pathway and endows it with cold hypersensitivity.<sup>28</sup> Conversely, *Hif1a*-deficient mice exhibited more pronounced nociceptive responses to thermal stimuli in manifold rodent pain models.<sup>27</sup> Moreover, ischemic preconditioning by tourniquet inflation on the limb significantly reduces pain and morphine consumption after orthopedic surgeries.<sup>29,30</sup>

Postoperative pain is predominantly characterized by ongoing spontaneous pain and pain on motion. With the DWB system, we captured those clinically relevant postoperative guarding behaviors and relief postures during free movements, which were shown as reduced weight-bearing and paw print areas of the operated paw after the surgery. However, no apparent effect of PIC using roxadustat on spontaneous pain-like behaviors was detected in our model. As the mechanisms underlying the development of postoperative pain involve complex pathways,<sup>31</sup> the ineffectiveness of PIC may be explained by a larger contribution of other sensitization mechanisms to the nociceptive system, rather than the



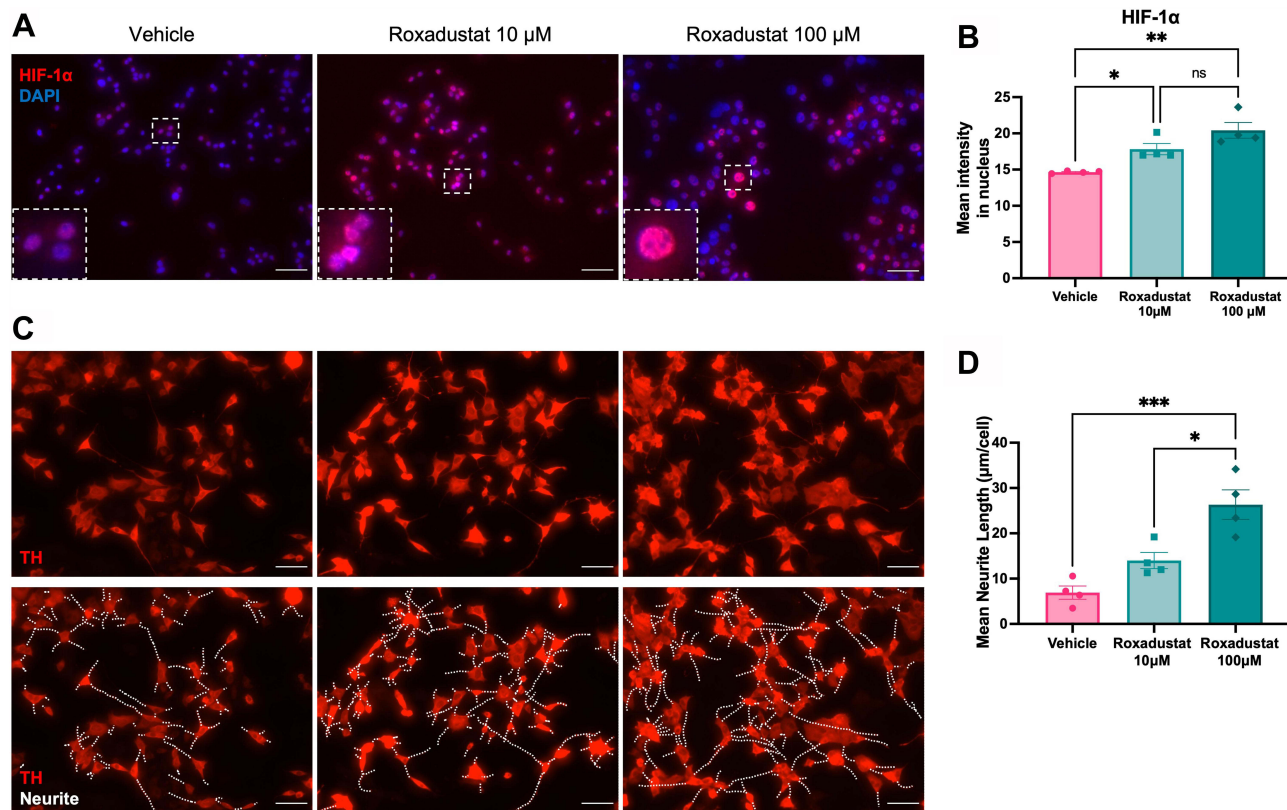


**Figure 5** Roxadustat dose dependently increased the nuclear translocation of HIF-1 $\alpha$  and TH-positive sympathetic neurite length of nerve growth factor-differentiated PC12 cells.

**Notes:** (A) Representative images of HIF-1 $\alpha$  with 4',6-diamidino-2-phenylindole in PC12 cells treated with roxadustat (10  $\mu$ M, 100  $\mu$ M) or vehicle on day 2. Scale bar = 50  $\mu$ m. Inserts display enlarged views of nuclear translocation of HIF-1 $\alpha$ . (B) Mean intensity of HIF-1 $\alpha$  in the nucleus ( $n = 4$  per group). (C) Representative images of TH<sup>+</sup> neurites in PC12 cells treated with roxadustat (10  $\mu$ M, 100  $\mu$ M) or vehicle on day 2. Scale bar = 50  $\mu$ m. (D) Mean neurite length of TH-positive PC12 cells ( $n = 4$  per group). Data are expressed as mean  $\pm$  SEM, assessed by one-way ANOVA with Tukey's multiple comparisons test. \* $P < 0.05$ , \*\* $P < 0.01$ , \*\*\* $P < 0.001$ .

**Abbreviations:** HIF-1 $\alpha$ , hypoxia-inducible factor 1-alpha; TH, tyrosine hydroxylase; ns, not significant.

hypoxic response mechanisms. Cumulatively, the involvement of the hypoxic response mechanisms in the development of pathological pain may be dependent on the type and underlying cause of pain. The effectiveness of PIC may also depend on the timing and mode of ischemic conditioning.

## PIC and Postoperative Local Sudomotor Dysfunction

Strikingly impaired local sudomotor function was observed around the surgical site in our restraint stress-induced sweating assay 3 weeks after deep hind paw incision, long after wound healing and easing of spontaneous pain-like behaviors. As the local sweating stimulated by systemic pilocarpine administration was comparable to that in naïve mice, the secretory function of eccrine gland cells may be undamaged even after surgical insults. Considering our immunohistochemical findings, the observed local sudomotor dysfunction could be attributable to the surgery-induced sympathetic denervation around the eccrine glands adjacent to the wound. Nevertheless, impeded local sweating has also been observed in mouse models of nerve injury and limb fracture, in which the association with post-traumatic processes leading to CRPS was implied.<sup>32</sup> Unexpectedly, our 3D immunohistochemistry data revealed a protective effect of PIC against this sudomotor dysfunction by facilitating sympathetic innervation to the eccrine glands around the wound.

A previous in vitro study has reported that HIF-1 regulates the gene expression of tyrosine hydroxylase (*Th*), a rate-limiting enzyme in the catecholamine biosynthesis in sympathetic neurons, via interactions with the specific hypoxia-responsive element in the proximal region of the *Th* promoter.<sup>33</sup> Another study using *Hif1a* conditional knockout mice has demonstrated a prerequisite of HIF-1 in sympathetic neurogenesis.<sup>34</sup> Beneficial roles of PHD inhibition in the nervous system under deleterious circumstances via stabilization of HIF-1 $\alpha$  have also been reported in vivo<sup>35</sup> and

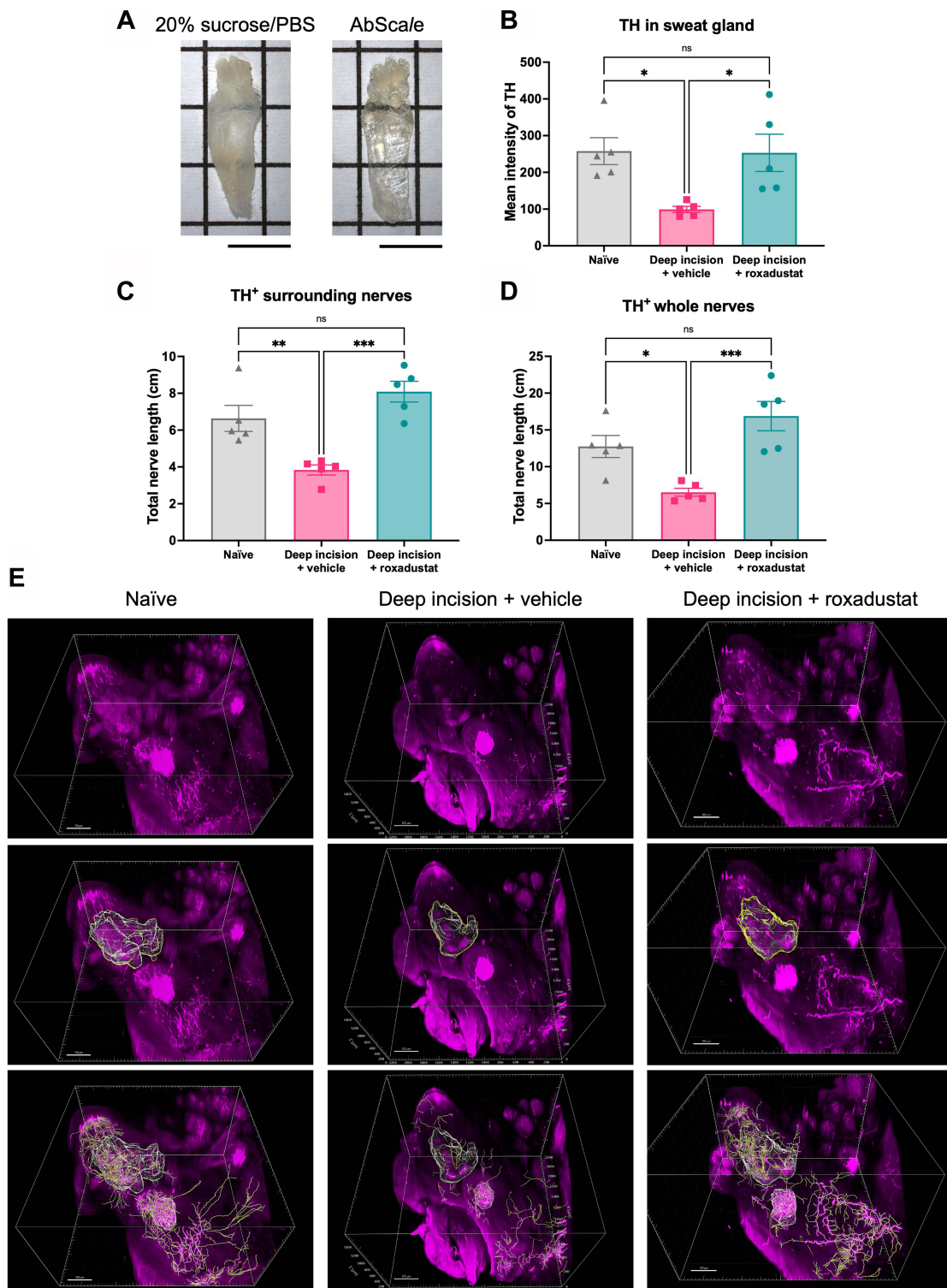


**Figure 6** Perioperative PIC using roxadustat significantly mitigated the surgery-induced sympathetic denervation.

**Notes:** (A) Representative photograph displaying the hind paw skin sample before and after the AbScale tissue-clearing method. Scale bar = 5 mm. (B) Mean intensity of TH immunoreactivity in the eccrine glands in the operated hind paws ( $n = 5$  per group). Total length of TH-positive nerve fibers surrounding (C) and within and around (D) the eccrine glands in the ipsilateral hind paws of naïve, deep incision + vehicle and deep incision + roxadustat mice ( $n = 5$  per group) on POD 21. (E) Representative images of skin samples adjacent to surgical wounds from ipsilateral hind paws with AbScale labeling of TH. Upper panels display stacked images without 3D rendering. Middle panels display stacked images with 3D rendering of the main eccrine glands. Bottom panels display stacked images with 3D rendering of the main eccrine glands and TH-positive nerve fibers within and around the eccrine glands. Scale bar = 300  $\mu\text{m}$ . Data are expressed as mean  $\pm$  SEM, assessed by one-way ANOVA with Tukey's multiple comparisons test. \* $P < 0.05$ , \*\* $P < 0.01$ , \*\*\* $P < 0.001$ .

**Abbreviations:** PIC, pharmacological ischemic conditioning; TH, tyrosine hydroxylase; POD, postoperative day; ns, not significant.

in vitro.<sup>19,36</sup> Consistently, our in vitro data using sympathetically differentiated PC12 cells proved that roxadustat treatment facilitated neurite growth by activating HIF-1 pathways. In addition, anti-apoptotic effects of PHD inhibitors on sympathetic neurons have also been reported.<sup>37</sup>

Thus, PIC exerts a protective effect against surgery-induced sympathetic denervation by activating the PHD–HIF hypoxic response pathways in the sympathetic nervous system.

## Hypoxic Response Pathway and Sympathetic Derangement in Postoperative CRPS

Our model did not fully reproduce CRPS-like manifestations other than sudomotor defects, such as long-lasting pain and peripheral vasomotor abnormalities. Hence, whether the observed local sudomotor impairment is veritably reflecting the pathogenesis of postoperative CRPS is unclear. However, our data revealed that the sudomotor dysfunction was attributable to the sympathetic denervation adjacent to the wound, which resembles the pathology in patients with CRPS with local sudomotor impairment.<sup>38</sup> Several hypotheses for peripheral nerve damage in CRPS have been postulated, including local pressure from edema in the affected limb, retrograde degeneration, and neurogenic inflammation.<sup>39</sup> Additionally, local symptoms of sympathetic and trophic changes can lead to endothelial dysfunction, and nerves may also be damaged through microvascular ischemia from resultant oxidative stress.<sup>40</sup>

Considering the pivotal role of hypoxic response mechanisms in regulating the sympathetic nervous system, the therapeutic effects of PIC demonstrated in this study may help to elucidate the pathology of sympathetic derangement in CRPS. During normal wound healing processes, the local restoration of tissue oxygenation terminates the activation of hypoxic response pathways via the negative feedback loop by upregulating oxygen-dependent PHD activities.<sup>41</sup> However, prolonged tissue hypoxia beyond the adaptive capacity of the hypoxic response system may lead to irreversible sympathetic denervation. Conversely, excessive activation of the hypoxia response pathways might potentially result in disproportionate sympathetic overgrowth, accelerating sympathetic hyperactivity that can be observed in a subset of patients with CRPS. Cumulatively, the sympathetic derangements in postoperative CRPS can be partly due to dysregulation of the hypoxic response mechanisms. Restoration of normal sympathetic innervation after tissue injury may require an early recovery of local oxygenation and properly orchestrated hypoxic responses.

In addition to sympathetic derangement, a dramatic hypertrophic profile of cutaneous vasculature was also observed in patients with CRPS.<sup>38</sup> An in vivo study using murine hypertension models found that roxadustat ameliorated hypertension and organ injury (eg, vascular thickening, cardiac hypertrophy, and kidney injury) via stabilization of HIF1 $\alpha$  and subsequent targeting of angiotensin receptors and oxidative stresses.<sup>42</sup> Conversely, hypertension has been reported by several clinical studies as one of the adverse events when roxadustat was administered for the treatment of renal anemia.<sup>43</sup> As sudomotor dysfunction could also result from an impaired microvascular perfusion,<sup>44</sup> it might be informative to monitor the blood pressure and observe the cutaneous microcirculation throughout the experiment. However, to fully explore and evaluate the therapeutic potential of the hypoxic response pathways in the progression to CRPS, further investigations are warranted.

## Limitations and Future Works

This study has some limitations.

First, the deep hind paw incision model in mice has an imperfect translatability to human biological responses to surgical procedure. Although this model reproduced many key aspects of surgical trauma, such as massive inflammation, tissue hypoxia, and behavioral alterations, it has a relatively shorter operative time and is less invasive. As patients undergoing orthopedic surgeries (eg, fracture fixation surgeries) are at a high risk of postoperative CRPS,<sup>45</sup> studies involving the application of PIC to orthopedic surgery models would be more informative. Additionally, the species-to-species differences, especially regarding the pathogenesis of sudomotor dysfunction, must also be considered. Different from rodents, the eccrine glands are not only concentrated in the plantar surface but also broadly distributed throughout the body in humans.<sup>46</sup> Therefore, the effect of surgical traumas and PIC on local sympathetic innervation and sudomotor function can be different in humans. As only male mice were used in the current study to avoid possible effects of the estrous cycle on basal body temperature and sudomotor function,<sup>47</sup> additional studies on female mice are also needed to detect the presence of sex differences.

Second, we qualitatively demonstrated the occurrence of tissue hypoxia in the surgical wound on POD 1 via pimonidazole adduct immunohistochemistry. To study the association between the degree of tissue hypoxia and postoperative pain or sudomotor dysfunction, it would be more informative to continuously monitor the tissue hypoxia by quantitative measurements (eg, oxygen-sensitive microelectrode or bioluminescence imaging reporters).<sup>9,48</sup>

Third, the secretory function of local eccrine gland cells seemed to be intact after surgical insults, as shown in the pilocarpine-induced perspiration (Figure 4D and E), where the muscarinic M3 receptors are directly stimulated. As we have identified PHD2 in eccrine gland cells (Supplementary Figure S2), where the expression of HIF-1 has also been previously described,<sup>49</sup> further studies are also required to validate whether PIC using PHD inhibitors also alters the secretory function by affecting hypoxia response mechanisms in eccrine gland cells.

Fourth, perioperative administration of roxadustat was selected in this study to maximize its hypoxia-mimetic effects throughout the time course of perioperative periods. The effects of PIC on these postoperative symptoms when roxadustat is solely administered pre-emptively or postoperatively should be investigated. Further studies on other PIC agents, such as iron chelators, and non-PIC, such as tourniquet inflation on the limb, would also be worthwhile.

## Conclusion

Perioperative PIC with roxadustat did not ease postoperative pain-like behaviors but alleviated surgery-induced sudomotor impairment by promoting sympathetic innervation to the eccrine glands around the wound. Hypoxic response mechanisms may be involved in the pathogenesis of local functional impairments in surgical wounds, and PIC may have therapeutic benefits for surgery-induced local sympathetic disorders.

## Acknowledgments

The authors thank the Collaborative Research Resources, Keio University School of Medicine, for its technical assistance. The authors are also grateful to Dr Atsushi Miyawaki and Dr Hiroshi Hama at the RIKEN Center for Brain Science for their assistance with the AbScale tissue-clearing method.

## Author Contributions

All authors have

1. Made a significant contribution to this work reported, whether in the conception, study design, execution, acquisition of data, analysis and interpretation, or in all these areas.
2. Drafted or written, or substantially revised or critically reviewed this article.
3. Agreed on the journal to which this article will be submitted.
4. Reviewed and agreed on all versions of this article before submission.
5. Agreed to take responsibility and be accountable for the contents of this article.

## Funding

This work was supported by the JSPS KAKENHI [grant number JP19K18252, Tomoko Toramaru] and Keio University Doctorate Student Grant-in-Aid Program from Ushioda Memorial Fund [Fanglin Lu]. The sponsors were not involved in any of the stages from study design to submission of the paper for publication.

## Disclosure

Jungo Kato is a member of the Patient Monitoring Strategic Advisory Board of Medtronic (USA). The remaining authors declare that they have no known competing financial interests or personal relationships that could have appeared to influence the work reported in this paper.

## References

1. Meara JG, Leather AJ, Hagander L, et al. Global surgery 2030: evidence and solutions for achieving health, welfare, and economic development. *Surgery*. 2015;158(1):3–6. doi:10.1016/j.surg.2015.04.011



2. Glare P, Aubrey KR, Myles PS. Transition from acute to chronic pain after surgery. *Lancet*. 2019;393(10180):1537–1546. doi:10.1016/S0140-6736(19)30352-6
3. Goebel A, Birklein F, Brunner F, et al. The Valencia consensus-based adaptation of the IASP complex regional pain syndrome diagnostic criteria. *Pain*. 2021;162(9):2346–2348. doi:10.1097/j.pain.0000000000002245
4. Carley ME, Chaparro LE, Choiniere M, et al. Pharmacotherapy for the prevention of chronic pain after surgery in adults: an updated systematic review and meta-analysis. *Anesthesiology*. 2021;135(2):304–325. doi:10.1097/ALN.0000000000003837
5. Li Z, Tseng PY, Tiwari V, et al. Targeting human Mas-related G protein-coupled receptor X1 to inhibit persistent pain. *Proc Natl Acad Sci U S A*. 2017;114(10):E1996–E2005. doi:10.1073/pnas.1615255114
6. Tiwari V, Anderson M, Yang F, et al. Peripherally acting mu-opioid receptor agonists attenuate ongoing pain-associated behavior and spontaneous neuronal activity after nerve injury in rats. *Anesthesiology*. 2018;128(6):1220–1236. doi:10.1097/ALN.0000000000002191
7. Tiwari V, He SQ, Huang Q, et al. Activation of micro-delta opioid receptor heteromers inhibits neuropathic pain behavior in rodents. *Pain*. 2020;161(4):842–855. doi:10.1097/j.pain.0000000000001768
8. Vaidya S, Shantanu PA, Tiwari V. Attenuation of ongoing neuropathic pain by peripheral acting opioid involves activation of central dopaminergic neurocircuitry. *Neurosci Lett*. 2021;754:135751. doi:10.1016/j.neulet.2021.135751
9. Kang S, Lee D, Theusch BE, Arpey CJ, Brennan TJ. Wound hypoxia in deep tissue after incision in rats. *Wound Repair Regen*. 2013;21(5):730–739. doi:10.1111/wrr.12081
10. Kim TJ, Fremel L, Park SS, Brennan TJ. Lactate concentrations in incisions indicate ischemic-like conditions may contribute to postoperative pain. *J Pain*. 2007;8(1):59–66. doi:10.1016/j.jpain.2006.06.003
11. Kido K, Gautam M, Benson CJ, Gu H, Brennan TJ. Effect of deep tissue incision on pH responses of afferent fibers and dorsal root ganglia innervating muscle. *Anesthesiology*. 2013;119(5):1186–1197. doi:10.1097/ALN.0b013e31829bd791
12. Sugiyama D, Kang S, Brennan TJ, Binshtok A. Muscle Reactive Oxygen Species (ROS) contribute to post-incisional guarding via the TRPA1 receptor. *PLoS One*. 2017;12(1):e0170410. doi:10.1371/journal.pone.0170410
13. Koban M, Leis S, Schultze-Mosgau S, Birklein F. Tissue hypoxia in complex regional pain syndrome. *Pain*. 2003;104(1):149–157. doi:10.1016/s0304-3959(02)00484-0
14. Watts ER, Walmsley SR. Inflammation and hypoxia: HIF and PHD isoform selectivity. *Trends Mol Med*. 2019;25(1):33–46. doi:10.1016/j.molmed.2018.10.006
15. Bernhardt WM, Gottmann U, Doyon F, et al. Donor treatment with a PHD-inhibitor activating HIFs prevents graft injury and prolongs survival in an allogeneic kidney transplant model. *Proc Natl Acad Sci U S A*. 2009;106(50):21276–21281. doi:10.1073/pnas.0903978106
16. Deguchi H, Ikeda M, Ide T, et al. Roxadustat markedly reduces myocardial ischemia reperfusion injury in mice. *Circ J*. 2020;84(6):1028–1033. doi:10.1253/circj.CJ-19-1039
17. Puzio M, Moreton N, O'Connor JJ. Neuroprotective strategies for acute ischemic stroke: targeting oxidative stress and prolyl hydroxylase domain inhibition in synaptic signalling. *Brain Disord*. 2022;5:100030. doi:10.1016/j.dscb.2022.100030
18. Banik RK, Woo YC, Park SS, Brennan TJ. Strain and sex influence on pain sensitivity after plantar incision in the mouse. *Anesthesiology*. 2006;105(6):1246–1253. doi:10.1097/00000542-200612000-00025
19. Wu K, Zhou K, Wang Y, et al. Stabilization of HIF-1 alpha by FG-4592 promotes functional recovery and neural protection in experimental spinal cord injury. *Brain Res*. 2016;1632:19–26. doi:10.1016/j.brainres.2015.12.017
20. Lu F, Kato J, Toramaru T, Sugai M, Zhang M, Morisaki H. Objective and quantitative evaluation of spontaneous pain-like behaviors using dynamic weight-bearing system in mouse models of postsurgical pain. *J Pain Res*. 2022;15:1601–1612. doi:10.2147/JPR.S359220
21. Hama H, Hioki H, Namiki K, et al. ScaleS: an optical clearing palette for biological imaging. *Nat Neurosci*. 2015;18(10):1518–1529. doi:10.1038/nn.4107
22. Faul F, Erdfelder E, Lang AG, Buchner A. G\*Power 3: a flexible statistical power analysis program for the social, behavioral, and biomedical sciences. *Behav Res Methods*. 2007;39(2):175–191. doi:10.3758/bf03193146
23. Dhillon S. Roxadustat: first global approval. *Drugs*. 2019;79(5):563–572. doi:10.1007/s40265-019-01077-1
24. Crowther M, Brown NJ, Bishop ET, Lewis CE. Microenvironmental influence on macrophage regulation of angiogenesis in wounds and malignant tumors. *J Leukoc Biol*. 2001;70(4):478–490. doi:10.1189/jlb.70.4.478
25. Schreml S, Szeimies RM, Prantl L, Karrer S, Landthaler M, Babilas P. Oxygen in acute and chronic wound healing. *Br J Dermatol*. 2010;163(2):257–268. doi:10.1111/j.1365-2133.2010.09804.x
26. Lim TK, Shi XQ, Johnson JM, et al. Peripheral nerve injury induces persistent vascular dysfunction and endoneurial hypoxia, contributing to the genesis of neuropathic pain. *J Neurosci*. 2015;35(8):3346–3359. doi:10.1523/jneurosci.4040-14.2015
27. Kanngiesser M, Mair N, Lim HY, et al. Hypoxia-inducible factor 1 regulates heat and cold pain sensitivity and persistence. *Antioxid Redox Signal*. 2014;20(16):2555–2571. doi:10.1089/ars.2013.5494
28. Miyake T, Nakamura S, Zhao M, et al. Cold sensitivity of TRPA1 is unveiled by the prolyl hydroxylation blockade-induced sensitization to ROS. *Nat Commun*. 2016;7:12840. doi:10.1038/ncomms12840
29. Memtsoudis SG, Stundner O, Yoo D, et al. Does limb preconditioning reduce pain after total knee arthroplasty? A randomized, double-blind study. *Clin Orthop Relat Res*. 2014;472(5):1467–1474. doi:10.1007/s11999-013-3106-4
30. Orban JC, Levraut J, Gindre S, et al. Effects of acetylcysteine and ischaemic preconditioning on muscular function and postoperative pain after orthopaedic surgery using a pneumatic tourniquet. *Eur J Anaesthesiol*. 2006;23(12):1025–1030. doi:10.1017/s026502150600086x
31. Pogatzki-Zahn EM, Segelcke D, Schug SA. Postoperative pain—from mechanisms to treatment. *Pain Rep*. 2017;2(2):e588. doi:10.1097/PR9.0000000000000588
32. Guhl C, Birklein F, Hirsch S. Sweating disorders in mice with and without nerve lesions. *Eur J Pain*. 2019;23(4):835–842. doi:10.1002/ejp.1352
33. Schnell PO, Ignacak ML, Bauer AL, Striet JB, Paulding WR, Czyzyk-Krzeska MF. Regulation of tyrosine hydroxylase promoter activity by the von Hippel-Lindau tumor suppressor protein and hypoxia-inducible transcription factors. *J Neurochem*. 2003;85(2):483–491. doi:10.1046/j.1471-4159.2003.01696.x
34. Bohuslavova R, Cerychova R, Papousek F, et al. HIF-1 alpha is required for development of the sympathetic nervous system. *Proc Natl Acad Sci U S A*. 2019;116(27):13414–13423. doi:10.1073/pnas.1903510116
35. Smaila BD, Holland SD, Babaeijandaghi F, Henderson HG, Rossi FMV, Ramer MS. Systemic hypoxia mimicry enhances axonal regeneration and functional recovery following peripheral nerve injury. *Exp Neurol*. 2020;334:113436. doi:10.1016/j.expneurol.2020.113436



36. Singh A, Wilson JW, Schofield CJ, Chen R. Hypoxia-inducible factor (HIF) prolyl hydroxylase inhibitors induce autophagy and have a protective effect in an in-vitro ischaemia model. *Sci Rep.* 2020;10(1):1597. doi:10.1038/s41598-020-58482-w
37. Johansen JL, Sager TN, Lotharius J, et al. HIF prolyl hydroxylase inhibition increases cell viability and potentiates dopamine release in dopaminergic cells. *J Neurochem.* 2010;115(1):209–219. doi:10.1111/j.1471-4159.2010.06917.x
38. Albrecht PJ, Hines S, Eisenberg E, et al. Pathologic alterations of cutaneous innervation and vasculature in affected limbs from patients with complex regional pain syndrome. *Pain.* 2006;120(3):244–266. doi:10.1016/j.pain.2005.10.035
39. Geertzen JH, Bodde MI, van den Dungen JJ, Dijkstra PU, den Dunnen WF. Peripheral nerve pathology in patients with severely affected complex regional pain syndrome type I. *Int J Rehabil Res.* 2015;38(2):121–130. doi:10.1097/mrr.0000000000000096
40. Coderre TJ, Bennett GJ. Objectifying CRPS-I. *Pain.* 2008;138(1):3–4. doi:10.1016/j.pain.2008.06.006
41. Foxler DE, Bridge KS, Foster JG, et al. A HIF-LIMD1 negative feedback mechanism mitigates the pro-tumorigenic effects of hypoxia. *EMBO Mol Med.* 2018;10(8). doi:10.15252/emmm.201708304
42. Yu J, Wang S, Shi W, et al. Roxadustat prevents Ang II hypertension by targeting angiotensin receptors and eNOS. *JCI Insight.* 2021;6(18). doi:10.1172/jci.insight.133690
43. Abdelazeem B, Shehata J, Abbas KS, et al. The efficacy and safety of roxadustat for the treatment of anemia in non-dialysis dependent chronic kidney disease patients: an updated systematic review and meta-analysis of randomized clinical trials. *PLoS One.* 2022;17(4):e0266243. doi:10.1371/journal.pone.0266243
44. Gandecka A, Araszkievicz A, Pilacinski S, Wierusz-Wysocka B, Zozulinska-Ziolkiewicz D. The relationship between sudomotor function and skin microvascular reactivity in individuals with type 1 diabetes of long duration. *Microvasc Res.* 2018;120:84–89. doi:10.1016/j.mvr.2018.07.002
45. Goh EL, Chidambaram S, Ma D. Complex regional pain syndrome: a recent update. *Burns Trauma.* 2017;5:2. doi:10.1186/s41038-016-0066-4
46. Kamberov YG, Karlsson EK, Kamberova GL, et al. A genetic basis of variation in eccrine sweat gland and hair follicle density. *Proc Natl Acad Sci U S A.* 2015;112(32):9932–9937. doi:10.1073/pnas.1511680112
47. Ratko M, Habek N, Kordic M, Dugandzic A. The use of infrared technology as a novel approach for studies with female laboratory animals. *Croat Med J.* 2020;61(4):346–353. doi:10.3325/cmj.2020.61.346
48. Godet I, Doctorman S, Wu F, Gilkes DM. Detection of hypoxia in cancer models: significance, challenges, and advances. *Cells.* 2022;11(4):686. doi:10.3390/cells11040686
49. Rosenberger C, Solovan C, Rosenberger AD, et al. Upregulation of hypoxia-inducible factors in normal and psoriatic skin. *J Invest Dermatol.* 2007;127(10):2445–2452. doi:10.1038/sj.jid.5700874

### Publish your work in this journal

The Journal of Pain Research is an international, peer reviewed, open access, online journal that welcomes laboratory and clinical findings in the fields of pain research and the prevention and management of pain. Original research, reviews, symposium reports, hypothesis formation and commentaries are all considered for publication. The manuscript management system is completely online and includes a very quick and fair peer-review system, which is all easy to use. Visit <http://www.dovepress.com/testimonials.php> to read real quotes from published authors.

Submit your manuscript here: <https://www.dovepress.com/journal-of-pain-research-journal>